UvA-DARE (Digital Academic Repository)

Improving Ammonia Production Using Zeolites

Matito-Martos, I.; García-Reyes, J.; Martin-Calvo, A.; Dubbeldam, D.; Calero, S.

[Link to publication](#)

THE JOURNAL OF
PHYSICAL CHEMISTRY C

Cite This: *J. Phys. Chem. C* 2019, 123, 18475−18481

Article

pubs.acs.org/JPCC

Improving Ammonia Production Using Zeolites

I. Matito-Martos,[†] J. García-Reyes,[†] A. Martin-Calvo,*,[†] D. Dubbeldam,[‡] and S. Calero*,[†]

[†]Department of Physical, Chemical, and Natural Systems. University Pablo de Olavide, 41013 Sevilla, Spain
[‡]Van't Hoff Institute for Molecular Sciences. University of Amsterdam, 1090 GD Amsterdam, The Netherlands

S *Supporting Information*

ABSTRACT: Ammonia is one of the most important compounds in the chemical industry as it is the main raw material in the production of fertilizers. Its production is achieved using the Haber−Bosch process, where nitrogen and hydrogen react in the presence of a catalyst producing a mixture containing ammonia. In this work we use molecular simulations to study the effect of confinement on the ammonia synthesis reaction in pure silica zeolites FER, MOR, MFI, BEA, LTA, and FAU. We calculated adsorption isotherms and isobars of the components resulting from the reaction for a wide range of values of pressure and temperature. The removal of the resulting ammonia will keep the equilibrium of the reaction favoring ammonia formation at lower values of pressure than in conventional plants. Among the studied zeolites, FAU and ITQ-29 are preferred for ammonia storage because of their higher adsorption capacity. The effect of confinement is proven to increase ammonia production, being the zeolites with the narrowest pores (FER and MFI) the ones that exhibit the highest conversion of the reactants. Besides, we found that the optimal working conditions for the production process in confinement are 573 K and 200 bar. At these particular conditions, the production of ammonia increases without the addition of any extra operational costs to the process.
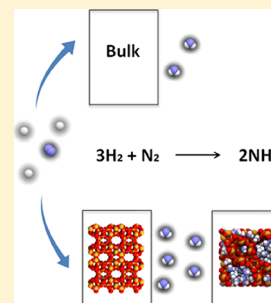
INTRODUCTION

The worldwide production of ammonia is among the largest within the chemical industry as it is probably the most important chemical in the world.[1,2] Synthetic ammonia is the main raw material in the production of fertilizers (80% of produced ammonia), nitric acid, urea plants, melamine, explosives, dyes, and plastics.[3,4] On a large scale, the industrial synthesis of ammonia is almost entirely produced by the Haber−Bosch process. This process generates a mixture of hydrogen, nitrogen, and carbon dioxide by burning fossil fuels with air and water. Once carbon dioxide is removed from the mixture, nitrogen and hydrogen react in the presence of a catalyst (typically iron), producing a diluted ammonia-gas stream that needs to be recovered. To break the strong bond of nitrogen, a temperature above 400 K is required. Additionally, high values of pressure (between 200 and 1000 bar) are used to enhance the production rate.[5] Only about 15% of synthesis gas is converted to ammonia each time in the reaction, requiring the gases to pass multiple times over the catalyst bed to achieve full conversion.[6] The synthesis of ammonia is highly exothermic. Therefore, long times are needed in order to reach equilibrium at high values of temperature. The activation energy of the reaction at room temperature is also too high, thus reducing drastically the reaction rate. Increasing pressure, reducing temperature, and at the same time using a catalyst will favor the proportion of ammonia yielded in the mixture. The removal of the product from the batch is also essential to ensure and keep the equilibrium in favor of ammonia formation. This way, ammonia can be synthesized at lower values of pressure than in conventional plants.[7,8]

On a very large scale, ammonia is traditionally separated from the other components of the reaction by condensation,[5] while on small and intermediate scales it can also be separated with gas absorbers.[9−11] However, high investments and operating costs are the main drawbacks of these techniques.[9−11] Separation and recovery of gaseous ammonia by adsorption is well known but has not been extensively applied. From the industrial application point of view, the selectivity, adsorption, and regeneration capacity of the adsorbent are of key importance.[9,11,12] The most studied materials for this purpose are MOFs, zeolites, and COFs, whose uptake capacity at room temperature and 1 bar partial pressure of ammonia could reach up to 105 mg/g (MOFs), 130 mg/g (zeolites), and 272 mg/g (COFs).[13−16] Here, we will focus on zeolites because they are the most commonly used at the industrial level for their low cost and high durability. Only a few zeolites are reported to have fair values of adsorption at the pressure and temperature conditions of the industrial gas stream.[17−21] In particular, 13X, 4A, and 5A zeolites, all of them containing extra-framework cations, are reported as the best candidates.[4,16,22] Nevertheless, it is known that the selective adsorption of ammonia is easier to achieve in the absence of water. Therefore, and to avoid intermediate steps in the industrial process, the use of pure silica zeolites seems promising for their hydrophobic nature.

Besides the selection of the optimal material, we need to take into account the effect of confinement on the chemical reaction equilibrium. To the best of our knowledge, there is not much information in this regard.[23−28] A previous study on activated carbons concluded that the yield in the pores is mainly determined by the increased density of the adsorbates. The

selectivity of the material for one of the reactants over the other is also an important factor at low pressure and/or temperature, but not at the high values of pressure and temperature considered at the industrial working conditions of the process. The yield of the ammonia reaction in the pores is not as sensitive to variations in temperature as to changes in density within the pore phase.[28]

■ METHODS

This work aims to improve the production of ammonia from the standard Haber−Bosch process by an efficient recovery of the gas using zeolites. For this purpose, molecular simulations are employed to analyze the performance of pure silica FER, MOR, BEA, MFI, LTA (ITQ-29), and FAU zeolites. We select these structures because they are currently used in the chemical and petrochemical industry.

We use the RASPA software package to simulate adsorption in zeolites.[29] In particular, we calculate isotherms and isobars with Monte Carlo (MC) simulations in the grand canonical ensemble (GCMC). In this ensemble, chemical potential, volume, and temperature are kept fixed. The chemical potential is related to pressure through the Peng−Robinson equation and the fugacity coefficient. Absolute adsorption values are converted into excess adsorption when comparing to experimental data.[30] Our simulations consist of 2.5×10^4 initialization cycles, 2.5×10^4 equilibration cycles, and 2×10^5 production cycles. Initialization cycles are used in MC to quickly equilibrate the position of the atoms in the system, while equilibration cycles are used to measure the biasing factors. Within each cycle, random trial moves are applied to a randomly selected molecule from the system. These moves are rotation, translation, regrow, insertion/deletion, and identity change (in the case of mixtures). The Continuous Fractional Component Monte Carlo method (CFCMC) is an algorithm used to improve the efficiency of ensembles where the number of molecules varies, as it allows increasing the number of successfully inserted molecules.[29,31−33] To deal with the ammonia synthesis reaction, we use a combination of CFCMC and the Reactive Monte Carlo method (RxMC). This method allows computing equilibrium properties for chemically reacting fluids.[34,35] RxMC extends the GCMC ensuring that the chemical reaction equilibria between reactants and products is maintained. This is achieved by sampling forward and backward the reaction, using MC moves. "Reaction" moves are also applied. Reactants are removed and products are inserted in the system in such a way that an equilibrium distribution is obtained. To perform RxMC simulations, the input of the intermolecular potentials and the ideal-gas partition function for the reactants and products are required along with the usual ensemble constants. The partition functions of the components of the reaction are taken from the literature[36,37] (Table S1 from the Supporting Information).

Host−guest and guest−guest interactions are modeled by Lennard-Jones (L-J) and Coulombic potentials, with point charges located at the center of the atoms of the system. Guest−guest L-J parameters are obtained by Lorentz−Berthelot mixing rules, while host−guest L-J parameters were fitted to reproduce experimental data. The Ewald summation method is used to calculate the Coulombic interactions with a relative precision of 1×10^{-6}. L-J and Coulombic potentials are cut and shifted at a cutoff distance of 12 Å. We use already published rigid models for hydrogen,[38] nitrogen,[39] and ammonia.[40] These models have been widely validated and reproduce characteristic properties of the gases such as the vapor−liquid equilibrium curve or the

vapor density. The molecule of hydrogen is defined as a single uncharged Lennard-Jones center that incorporates quantum corrections with a Feynman−Hibbs effective interaction potential. The molecules of nitrogen and ammonia are modeled with Lennard-Jones parameters, point charges in all their atoms, and a charged dummy atom without mass to mimic the polarity of the molecules. The zeolites used here vary in topology. FER and MOR have 2D systems of interconnected channels, BEA and MFI have 3D systems of interconnected channels, and FAU and LTA have 3D systems of large cavities surrounded by sodalites. Zeolites are considered as rigid frameworks. We use reported crystallographic positions of the atoms from Morris et al.[41] (FER), Gramlich[42] (MOR), Newsam[43] (BEA), van Koningsveld et al.[44] (MFI), Hriljac et al.[45] (FAU), and Corma et al.[46] (LTA-ITQ-29). The cell parameters of these zeolites are summarized in Table S2 from the Supporting Information.

All atoms of the structure have point charges assigned.[47] For the molecule of hydrogen, we define L-J interactions of the molecules with the silicon and oxygen atoms of the framework.[38] For nitrogen and ammonia, we use effective L-J parameters for the zeolites oxygen atom only (Ozeo).[48] These parameters are collected in Table 1.

Table 1. Lennard-Jones Parameters and Point Charges Used

atom 1	atom 2	ε/k_B (K)	σ (Å)	μ_{ij} (uma)	charge (e⁻)
Adsorbates					
H (H$_2$)	H (H$_2$)	36.733	2.958	1	0
N (N$_2$)	N (N$_2$)	38.298	3.306		−0.405
dummy (N$_2$)	dummy (N$_2$)				0.81
N (NH$_3$)	N (NH$_3$)	185	3.42		0
H (NH$_3$)	H (NH$_3$)				0.41
dummy (NH$_3$)	dummy (NH$_3$)				−1.23
Zeolites					
O (zeo)	O (zeo)				−0.393
Si (zeo)	O (zeo)				0.786
Adsorbates—Zeolites					
H (H$_2$)	O (zeo)	66.055	2.89	1.79	
H (H$_2$)	Si (zeo)	28.256	1.854	1.86	
N (N$_2$)	O (zeo)	60.58	3.261		
N (NH$_3$)	O (zeo)	160	3.125		

■ RESULTS AND DISCUSSION

Prior to the analysis of the adsorption of mixtures, we first evaluate the pure component adsorption in the zeolites at several working conditions. We calculate the loading of hydrogen, nitrogen, and ammonia in the zeolites at a pressure range of 10^{-6} bar to 100 bar and temperature from 80 to 300 K (Figures S1−S3 from the Supporting Information).

To enhance ammonia production, the idea is to separate this component from the other components of the mixture. Therefore, we look for the optimal combination of pressure and temperature, where the uptakes of hydrogen and nitrogen are low and the loading of ammonia is high. This information can be used to predict the most suitable operating conditions for the process. In particular, at 300 K and 100 bar, the loading of ammonia seems directly related to the available pore volume of the zeolites (FAU > LTA > BEA > MOR > MFI > FER). We found ammonia condensation inside the pores of the zeolites at most temperatures (Figure 1). The steepness of the isotherms at
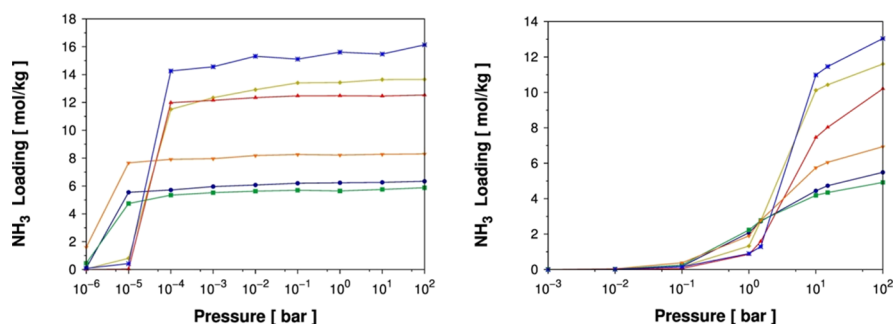
Figure 1. Ammonia adsorption at 140 K (left) and 300 K (right) in the zeolites under study: BEA (red), FAU (blue), FER (green), LTA (yellow), MFI (purple), and MOR (orange).

140 K in a narrow range of pressure indicates phase transition of ammonia. This only occurs for FAU, LTA, and maybe BEA at 300 K and requires much higher values of pressure. It is for this reason that the use of high temperature is very important for this particular process.

Before evaluating the effect of the zeolites on the reaction yield, we validate the models and force fields with the reaction of synthesis of ammonia in the bulk at several temperatures. Figure 2 compares the ammonia reaction yield obtained using RxMC
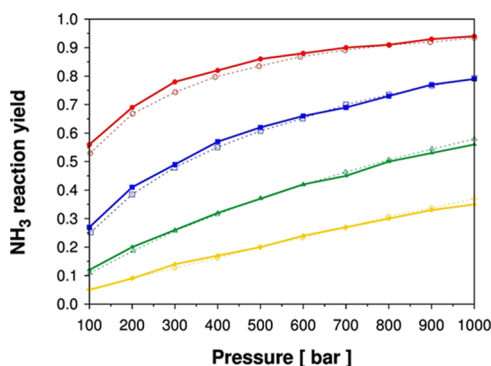

Figure 2. Ammonia mole fraction from the reaction of nitrogen and hydrogen at 573 K (red), 673 K (blue), 773 K (green), and 873 K (yellow). Comparison between calculated values (solid symbols and lines) and experimental data (open symbols and dashed lines).[49]

simulations with reported experimental values.[49] As seen in the figure, the highest ammonia reaction yield is obtained at 573 K for all partial pressures, with a maximum at 1000 bar, with nearly full formation of ammonia.

To obtain the highest reaction yield, one needs to take into account not only the temperature of the process but also the pressure (Figure 3). We compare our results at 100 and 200 bar with the experimental values from Haber.[50] As observed from the figure there is a perfect match between both sets of data, therefore we can extrapolate our conclusions from the experimental values of Haber. At 473 K, it is possible to get over 86% yield by increasing pressure from 1 to 200 bar. However, at this temperature, differences in the yields at 100 and 200 bar are not significant (5% difference). As Fritz Haber mentioned during his Nobel Lecture in 1920, an increase in pressure is only of interest if it considerably reduces the temperature of rapid conversion without creating technical difficulties.

The next step in this work is to investigate the effect of confinement on the equilibrium of the reaction of ammonia synthesis from nitrogen and hydrogen. To this aim, we
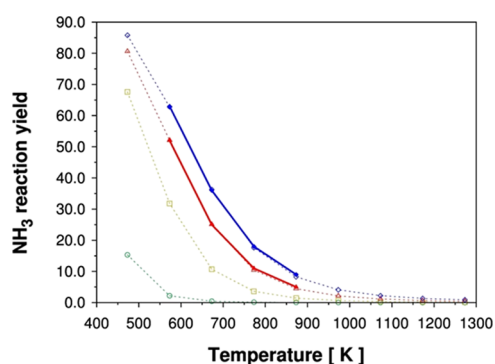
Figure 3. Calculated ammonia reaction yield at 100 bar (solid red triangles) and 200 bar (solid blue diamonds). Dashed lines and open symbols are the values reported by Haber during his Nobel Lecture in 1920,[50] including data at 1 bar (green circles) and 30 bar (orange squares).

performed MC simulations using the initial molar fractions of the components of the reaction previously obtained by RxMC simulations (Table S3). Instead of running new RxMC simulations, this reduces computational time. However, it has been previously validated that the results obtained will not vary between methods.[51]

As shown in Figure 4, the production of ammonia increases in all cases. This finding was previously reported for activated carbons by Turner et al.[28] with an increased yield of ammonia of about 40%, being the narrowest pores the responsible of the
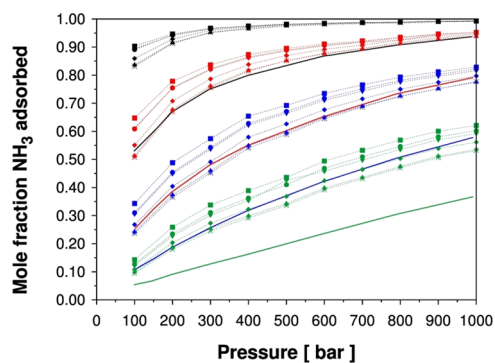

Figure 4. Mole fraction of adsorbed ammonia as a function of pressure. Solid lines represent the values in the bulk, while dashed lines and symbols are the values calculated in the zeolites: BEA (up triangles), FAU (asterisks), FER (squares), LTA (diamonds), MFI (circles), and MOR (down triangles). Colors refer to temperature: 873 K (green), 773 K (blue), 673 K (red), and 573 K (black).

largest improvement. As seen in the figure, the lower the pressure the larger the effect exerted by confinement on the ammonia production. The largest increase was observed at 673 K, with an enhanced yield of 51% at 200 bar in FER. The optimum value of temperature is 573 K with almost a full production of ammonia and constant values for the whole range of pressure studied. In the same tone as Turner et al., zeolites with smaller pore volume show the largest mole fraction of ammonia adsorbed (opposite trend than for the adsorption isotherms of the pure components). This behavior is expected, as the effect of confinement in the reaction will be reduced in zeolites with large pores. However, differences between zeolites are almost negligible at 573 K, with an average enhancement of about 17%. Table S4 from the Supporting Information, compares the absolute increment and the percentage of enhancement achieved with the zeolites compared to the results obtained in the bulk. At higher values of temperature (773 and 873 K), the percentages of enhancement seem higher; however, the absolute increment is much lower than at 573 or 673 K.

Based in our findings, 573 K and 200 bar provide the best balance of temperature and pressure for an efficient synthesis of ammonia. These operating conditions guarantee high ammonia production (between 91 and 94% ammonia adsorbed) without requiring substantial costs. Besides the reaction yields obtained within the materials, it is interesting to see the distribution of the molecules inside the structures. Because the adsorption of hydrogen and nitrogen is almost negligible at these conditions, we can analyze the distribution of the molecules of ammonia inside the zeolites with the average density profiles (Figures 5−7). These plots are obtained from the projection over the planes of the center of mass of the molecules adsorbed inside the pores of the zeolites.

The average density profiles of ammonia in FER and MOR (2D systems of interconnected channels) show that the molecules are preferably adsorbed in the smallest channels (5.4×4.2 and 4.8×3.5 Å in FER and 7.0×6.5 and 5.7×2.6 Å in MOR), being the side pockets of MOR the preferred location for this zeolite. FER is the structure with the narrowest channels and for this reason is the zeolite that provides the best improvement in the ammonia production. The preferred locations for the molecules of ammonia in BEA and MFI (3D systems of interconnected channels) are the intersections between channels. The molecules of ammonia are more confined in the channels of MFI (narrower) than in the channels of BEA (wider). FAU and ITQ-29 (3D systems of cages surrounded by sodalites) show homogeneous adsorption of ammonia distributed between the super cages and the sodalities of these zeolites. The homogeneity on the adsorption is a consequence of the large size of the cavities of these materials. As in the previous cases, the zeolite with the smallest cavities (ITQ-29) shows the highest concentration of molecules.

Figure 8 shows the adsorption of ammonia, nitrogen, and hydrogen at 573 K and 200 bar. It compares the results obtained when the reaction takes place ($NH_3/N_2/H_2$ 62.55511:9.36122:28.08367) with the expected mixture using the stoichiometry of the reaction in ideal conditions ($NH_3/N_2/H_2$ 33.3:16.7:50). Hydrogen and nitrogen adsorptions are lower in real conditions than the expected from the stoichiometric mixture; however, the adsorption of ammonia is largely increased in all zeolites. These results corroborate once more the positive effect of confinement on the production and recovery of ammonia. FAU and LTA topologies show the highest ammonia adsorption for both mixtures. Despite
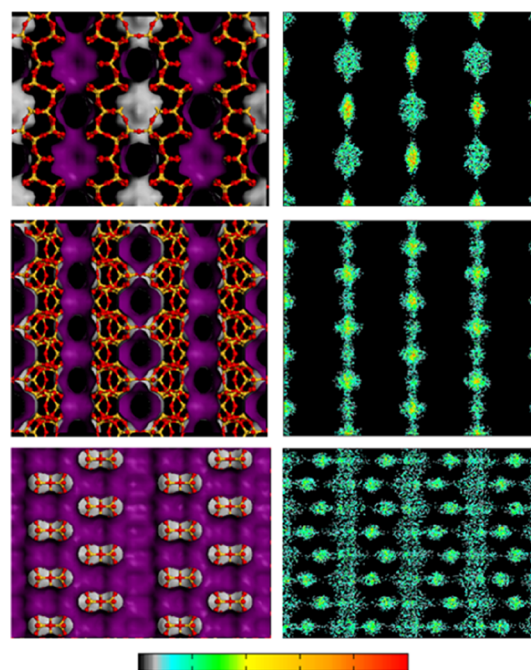

Figure 5. Average density profiles of ammonia inside the pores of the zeolites at 573 K and 200 bar (right). From top to bottom: *XY* and *XZ* views for FER and *YZ* view for MOR. The color gradation (black-blue-green-yellow-orange-red) indicates the less and most populated areas. To guide the view, we add a representation of the structures (left). The atomic structures are represented by the oxygen and silica atoms in red and yellow, respectively. Grid surfaces where the accessible part appears in purple and the non-accessible part is colored in gray are also depicted.
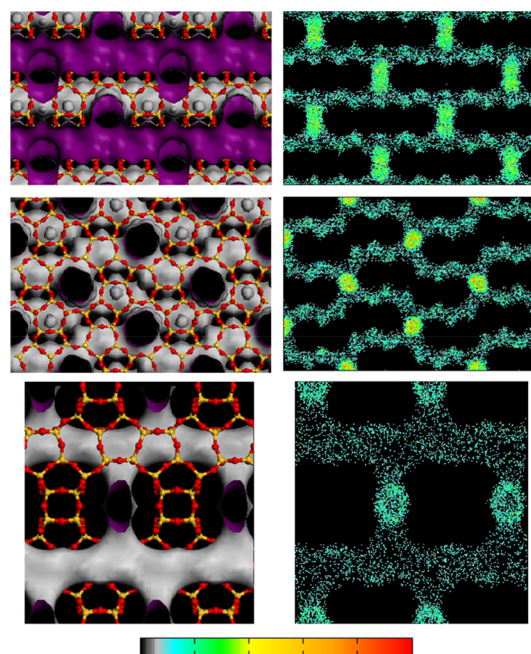
Figure 6. Average density profiles of ammonia inside the pores of the zeolites at 573 K and 200 bar (left). From top to bottom: *YZ* and *XZ* views for MFI and *YZ* view for BEA. The color gradation (black-blue-green-yellow-orange-red) indicates the less and most populated areas. To guide the view, we add a representation of the structures (left). The atomic structures are represented by the oxygen and silica atoms in red and yellow, respectively. Grid surfaces where the accessible part appears in purple and the non-accessible part is colored in gray are also depicted.
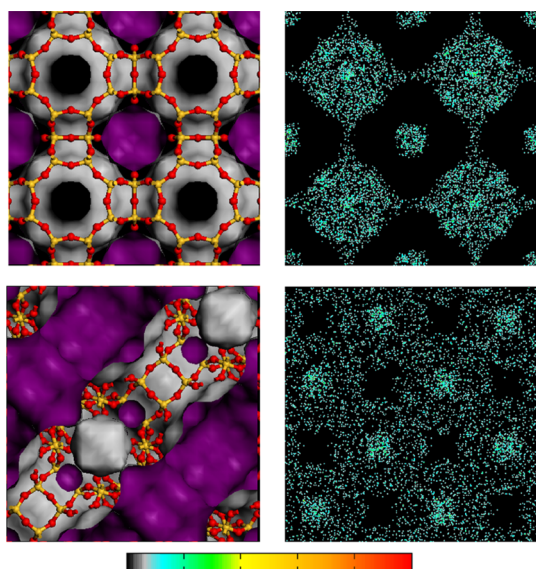
Figure 7. Average density profiles of ammonia inside the pores of the zeolites at 573 K and 200 bar (right). From top to bottom: *XY* views for LTA and FAU. The color gradation (black-blue-green-yellow-orange-red) indicates the less and most populated areas. To guide the view, we add a representation of the structures (left). The atomic structures are represented by the oxygen and silica atoms in red and yellow, respectively. Grid surfaces where the accessible part appears in purple and the non-accessible part is colored in gray are also depicted.
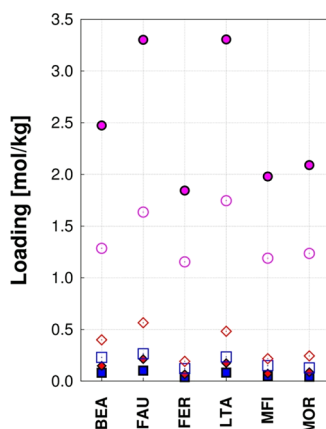

Figure 8. Adsorption of hydrogen (red), nitrogen (blue), and ammonia (pink) at 573 K and 200 bar from the mixture $NH_3/N_2/H_2$ with reactive (closed symbols) and stoichiometric (open symbols) proportions in the zeolites under study.

differences in ammonia uptakes follow similar trends, larger differences between zeolite behaviors are observed for the reactive than for the stoichiometric mixture.

We found in this work that the material with the highest ammonia capacity is different than the material with the highest ammonia formation. Therefore, the selection of the best performing material will depend on the criteria set for the application. Figure 9 shows the performance of the materials at 573 K and 200 bar in terms of their ammonia uptake and increment in the ammonia production. As observed from the figure, FER is the best zeolite in terms of ammonia production, while FAU and LTA have the largest adsorption capacity.
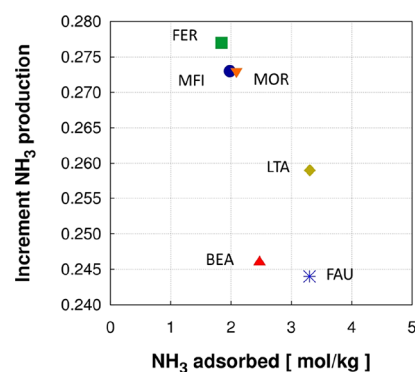
Figure 9. Comparison of the ammonia uptake and percentage of enhancement of ammonia production of the zeolites under study at 573 K and 200 bar in FER (green square), MOR (orange down-triangle), MFI (dark blue circle), BEA (red up-triangle), LTA (yellow diamond), and FAU (blue asterisk).

CONCLUSIONS

We carried out molecular simulations to study the performance of pure silica zeolites FER, MOR, BEA, MFI, LTA, and FAU in the production process of ammonia. Aiming to improve the yield of ammonia from its synthesis reaction, the effect of confinement was studied. Several working conditions were investigated for pressure up to 1000 bar and temperature ranging between 80 and 873 K. The need of working at a high temperature (above 400 K) was found to be needed, because otherwise a phase transition of ammonia to liquid ammonia occurs. The effect of confinement is proved to increase the ammonia production in all zeolites with special improvement in FER. However, in terms of ammonia capture, zeolites with the largest pore volume (FAU or LTA) show the highest adsorption capacity, proposing this material as the optimal candidate for ammonia recovery. The right balance of temperature and pressure (573 K and 200 bar) leads to the highest ammonia yield without implying high implementation costs. Therefore, depending on which step of the ammonia production we want to implement, a different material should be selected: FER to enhance the production and FAU for a better recovery of ammonia.

ASSOCIATED CONTENT

Ⓢ Supporting Information

The Supporting Information is available free of charge on the ACS Publications website at DOI: 10.1021/acs.jpcc.9b05366.

> Hydrogen, nitrogen, and ammonia pure component adsorption isotherms in zeolites at a pressure range between 10^{-6} bar and 10^2 bar and temperature from 80 to 300 K; ideal-gas partition functions for gases under study; cell parameters of zeolites used in this work; equilibrium molar fractions for the ammonia formation reaction in the bulk at several working conditions; and increment and percentage of enhancement of the ammonia fractions under confinement on each selected zeolite (PDF)

AUTHOR INFORMATION

Corresponding Authors
*E-mail: amarcal@upo.es (A.M.-C.).
*E-mail: scalero@upo.es (S.C.).
ORCID Ⓘ
I. Matito-Martos: 0000-0002-2107-0927
A. Martin-Calvo: 0000-0002-0284-6777

D. Dubbeldam: 0000-0002-4382-1509
S. Calero: 0000-0001-9535-057X

Notes

■ ACKNOWLEDGMENTS

■ REFERENCES

(1) Erisman, J. W.; Sutton, M. A.; Galloway, J.; Klimont, Z. How a Century of Ammonia Synthesis Changed the World. *Nat. Geosci.* **2008**, *1*, 636−639.

(2) Borlaug, N. E. *The Green Revolution Revisited and The Road Ahead*: Oslo, 2000.

(3) Smil, V. Detonator of the Population Explosion. *Nature* **1999**, *400*, 415.

(4) Helminen, J.; Helenius, J.; Paatero, E.; Turunen, I. Comparison of Sorbents and Isotherm Models for NH3-Gas Separation by Adsorption. *AIChE J.* **2000**, *46*, 1541−1555.

(5) Jennings, J. R. *Catalytic Ammonia Synthesis, Fundamental and Practice*; Twigg, M. V., Spencer, M. S., Eds.; Springer US: United States, 1991.

(6) Smil, V. *Enriching the Earth: Fritz Haber, Carl Bosch, and Transformation of World Food Production*; MIT Press: Massachusetts, 2002; Vol. *93*.

(7) Malmali, M.; Wei, Y.; McCormick, A.; Cussler, E. L. Ammonia Synthesis at Reduced Pressure via Reactive Separation. *Ind. Eng. Chem. Res.* **2016**, *55*, 8922−8932.

(8) Malmali, M.; Reese, M.; McCormick, A. V.; Cussler, E. L. Converting Wind Energy to Ammonia at Lower Pressure. *ACS Sustainable Chem. Eng.* **2018**, *6*, 827−834.

(9) Lavie, R. *Process for the Manufacture of Ammonia*, 1985.

(10) Hirai, H.; Komiyama, M.; Kurima, K.; Wada, K. Adsorbent for Use in Selective Gas Adsorption-Separation and a Process for Producing the Same. U.S. Patent 4,675,309 A, 1987.

(11) Knaebel, K. S. *Pressure Swing Adsorption System for Ammonia Synthesis*, Springer US: 1998.

(12) Isalski, W. H. Recovery of Hydrogen and Ammonia from Purge Gas. U.S. Patent 4,266,957 A, 1981.

(13) Britt, D.; Tranchemontagne, D.; Yaghi, O. M. Metal-Organic Frameworks with High Capacity and Selectivity for Harmful Gases. *Proc. Natl. Acad. Sci. U.S.A.* **2008**, *105*, 11623−11627.

(14) Jasuja, H.; Peterson, G. W.; Decoste, J. B.; Browe, M. A.; Walton, K. S. Evaluation of MOFs for air purification and air quality control applications: Ammonia removal from air. *Chem. Eng. Sci.* **2015**, *124*, 118−124.

(15) Doonan, C. J.; Tranchemontagne, D. J.; Glover, T. G.; Hunt, J. R.; Yaghi, O. M. Exceptional Amonia Uptake by a Covalent Organic Framework. *Nat. Chem.* **2010**, *2*, 235−238.

(16) Helminen, J.; Helenius, J.; Paatero, E. Adsorption Equilibria of Ammonia Gas on Inorganic and Organic Sorbents at 298.15 K. *J. Chem. Eng. Data* **2001**, *46*, 391−399.

(17) Boki, K.; Tanada, S.; Tsutsui, S.; Ohtani, N.; Yamasaki, R.; Nakamura, M. Characterization of adsorption of nitrogen and n-butane in microporous activated carbon. *J. Colloid Interface Sci.* **1987**, *115*, 286−287.

(18) Kuo, S.; Pedram, E. O.; Hines, A. L. Analysis of Ammonia Adsorption on Silica Gel Using the Modified Potential Theory. *J. Chem. Eng. Data* **1985**, *30*, 330−332.

(19) Coughlan, B.; McCann, W. A. Adsorption properties of zeolitic ruthenium and of chromium, iron and lanthanum mordenites. Part 1.-Equilibria and affinities. *J. Chem. Soc.* **1979**, *75*, 1969−1983.

(20) Shiralkar, V. P.; Kulkarni, S. B. Sorption of Ammonia in Cation-Exchanged Y Zeolites: Isotherms and State of Sorbed Molecules 1. *J. Colloid Interface Sci.* **1985**, *108*, 1.

(21) Hayhurst, D. T. Gas Adsorption by Some Natural Zeolites. *Chem. Eng. Commun.* **1980**, *4*, 729−735.

(22) Jaramillo, E.; Chandross, M. Adsorption of Small Molecules in LTA Zeolites. 1. NH3, CO2, and H2O in Zeolite 4A. *J. Phys. Chem. B* **2004**, *108*, 20155−20159.

(23) Trokhymchuk, A.; Pizio, O.; SokoŁowski, S. Solvation Force for an Associative Fluid in a Slit-like Pore. *J. Colloid Interface Sci.* **1996**, *178*, 436−441.

(24) Trokhymchuk, A.; Henderson, D.; Sokołowski, S. Structure of Chemically Reacting Particles near a Hard Wall from Integral Equations and Computer Simulations. *Can. J. Phys.* **1996**, *74*, 65−76.

(25) Pizio, O.; Henderson, D.; Soko-lowski, S. Density Profiles of Chemically Reacting Simple Fluids near Impenetrable Surfaces. *J. Phys. Chem.* **1995**, *99*, 2408−2411.

(26) Pizio, O.; Henderson, D.; Sokołowski, S. Adsorption of chemically reacting fluids on a crystalline surface. *Mol. Phys.* **1995**, *85*, 407−412.

(27) Müller, E. A.; Vega, L. F.; Gubbins, K. E.; Rull, L. F. Adsorption isotherms of associating chain molecules from Monte Carlo simulations. *Mol. Phys.* **1995**, *85*, 9−21.

(28) Turner, C. H.; Johnson, J. K.; Gubbins, K. E. Effect of Confinement on Chemical Reaction Equilibria: The Reactions 2NO ↔ (NO)2 and N2+ 3H2↔ 2NH3 in Carbon Micropores. *J. Chem. Phys.* **2001**, *114*, 1851−1859.

(29) Dubbeldam, D.; Calero, S.; Ellis, D. E.; Snurr, R. Q.; Dubbeldam, D.; Calero, S.; Ellis, D. E.; Snurr, R. Q. *RASPA: Molecular Simulation Software for Adsorption and Diffusion in Flexible Nanoporous Materials*, 2016; p 7022.

(30) Düren, T.; Sarkisov, L.; Yaghi, O. M.; Snurr, R. Q. Design of New Materials for Methane Storage. *Langmuir* **2004**, *20*, 2683−2689.

(31) Shi, W.; Maginn, E. J. Continuous Fractional Component Monte Carlo: An Adaptive Biasing Method for Open System Atomistic Simulations. *J. Chem. Theory Comput.* **2007**, *3*, 1451−1463.

(32) Shi, W.; Maginn, E. J. Improvement in Molecule Exchange Efficiency in Gibbs Ensemble Monte Carlo: Development and Implementation of the Continuous Fractional Component Move. *J. Comput. Chem.* **2008**, *29*, 2520−2530.

(33) Rosch, T. W.; Maginn, E. J. Reaction Ensemble Monte Carlo Simulation of Complex Molecular Systems. *J. Chem. Theory Comput.* **2011**, *7*, 269−279.

(34) Johnson, J. K.; Panagiotopoulos, A. Z.; Gubbins, K. E. Reactive canonical Monte Carlo. *Mol. Phys.* **1994**, *81*, 717−733.

(35) Smith, W. R.; Triska, B. The Reaction Ensemble Method for the Computer Simulation of Chemical and Phase Equilibria. I. Theory and Basic Examples. *J. Chem. Phys.* **1994**, *100*, 3019−3027.

(36) Poursaeidesfahani, A.; Hens, R.; Rahbari, A.; Ramdin, M.; Dubbeldam, D.; Vlugt, T. J. H. Efficient Application of Continuous Fractional Component Monte Carlo in the Reaction Ensemble. *J. Chem. Theory Comput.* **2017**, *13*, 4452−4466.

(37) Poursaeidesfahani, A.; Hens, R.; Rahbari, A.; Ramdin, M.; Dubbeldam, D.; Vlugt, T. J. H. Supporting Information for: Efficient Application of Continuous Fractional Component Monte Carlo in the Reaction Ensemble Partition Function of Serial Rx/CFC. *J. Chem. Theory Comput.* **2017**, *13*, 1−37.

(38) Deeg, K. S.; Gutiérrez-Sevillano, J. J.; Bueno-Pérez, R.; Parra, J. B.; Ania, C. O.; Doblaré, M.; Calero, S. Insights on the Molecular Mechanisms of Hydrogen Adsorption in Zeolites. *J. Phys. Chem. C* **2013**, *117*, 14374−14380.

(39) Martín-Calvo, A.; García-Pérez, E.; García-Sánchez, A.; Bueno-Pérez, R.; Hamad, S.; Calero, S. Effect of Air Humidity on the Removal of Carbon Tetrachloride from Air Using Cu-BTC Metal-Organic Framework. *Phys. Chem. Chem. Phys.* **2011**, *13*, 11165−11174.

(40) Zhang, L.; Siepmann, J. I. Development of the Trappe Force Field for Ammonia. *Collect. Czech. Chem. Commun.* **2010**, *75*, 577−591.

(41) Morris, R. E.; Weigel, S. J.; Henson, N. J.; Bull, L. M.; Janicke, M. T.; Chmelka, B. F.; Cheetham, A. K. A Synchrotron X-Ray Diffraction ,

Neutron Diffraction , 29Si MAS — NMR , and Computational Study of the Siliceous Form of Zeolite Ferrierite. *J. Am. Chem. Soc.* **1994**, *116*, 11849−11855.

(42) Gramlich, V. *Untersuchung Und Verfeinerung Pseudosymmetrischer Strukturen*; Juris: Zurich, 1971.

(43) Newsam, J. M. Structures of Dehydrated Potassium Zeolite L at 298 and 78 K and at 78 K Containing Sorbed Perdeuteriobenzene. *J. Phys. Chem.* **1989**, *93*, 7689−7694.

(44) van Koningsveld, H.; van Bekkum, H.; Jansen, J. C. On the Location and Disorder of the Tetrapropylammonium (TPA) Ion in Zeolite ZSM-5 with Improved Framework Accuracy. *Acta Crystallogr., Sect. B: Struct. Sci.* **1987**, *43*, 127−132.

(45) Hriljac, J. A.; Eddy, M. M.; Cheetham, A. K.; Donohue, J. A.; Ray, G. J. Powder Neutron Diffraction and 29Si MAS NMR Studies of Siliceous Zeolite-Y. *J. Solid State Chem.* **1993**, *106*, 66−72.

(46) Corma, A.; Rey, F.; Rius, J.; Sabater, M. J.; Valencia, S. Supramolecular Self-Assembled Molecules as Organic Directing Agent for Synthesis of Zeolites. *Nature* **2004**, *431*, 287−290.

(47) García-Sánchez, A.; Ania, C. O.; Parra, J. B.; Dubbeldam, D.; Vlugt, T. J. H.; Krishna, R.; Calero, S. Transferable Force Field for Carbon Dioxide Adsorption in Zeolites. *J. Phys. Chem. C* **2009**, *113*, 8814.

(48) Martin-Calvo, A.; Gutiérrez-Sevillano, J. J.; Parra, J. B.; Ania, C. O.; Calero, S. Transferable Force Fields for Adsorption of Small Gases in Zeolites. *Phys. Chem. Chem. Phys.* **2015**, *17*, 24048−24055.

(49) Gillespie, L. J.; Beattie, J. A. The Thermodynamic Treatment of Chemical Equilibria in Systems Composed of Real Gases. I. An Approximate Equation for the Mass Action Function Applied to the Existing Data on the Haber Equilibrium. *Phys. Rev.* **1930**, *36*, 743−753.

(50) Haber, F. *The Synthesis of Ammonia from Its Elements. Nobel Lect.* 1920.

(51) Matito-Martos, I.; Rahbari, A.; Martin-Calvo, A.; Dubbeldam, D.; Vlugt, T. J. H.; Calero, S. Adsorption Equilibrium of Nitrogen Dioxide in Porous Materials. *Phys. Chem. Chem. Phys.* **2018**, *20*, 4189−4199.